Audio Engineering Society

Convention Paper

Presented at the 128th Convention
2010 May 22–25 London, UK

Considerations for the Optimal Location and Boundary Effects for Loudspeakers in an Automotive Interior

Roger Shively[1], Jeff Bailey[2], Jérôme Halley[3], Lars Kurandt[4], François Malbos[5], Gabriel Ruiz[6], and Alfred Svobodnik[7]

[1] Harman International, Novi, Michigan, USA
Roger.Shively@harman.com

[2] Harman International, Novi, Michigan, USA
Jeffrey.Bailey@harman.com

[3] Harman International, Karlsbad, Germany
Jerome.Halley@harman.com

[4] Harman International, Karlsbad, Germany
Lars.Kurandt@harman.com

[5] Harman International, Chateau du Loir, France
Francois.Malbos@harman.com

[6] Harman International, Bridgend, Wales, UK
Gabriel.Ruiz@harman.com

[7] Harman International, Vienna, Austria
Alfred.Svobodnik@harman.com

ABSTRACT

Referencing earlier work by the authors on the boundary effects in an automotive vehicle interior [1] on the mid-to-high frequency timbral changes in the sound field due to the proximity to loudspeakers of reflective, semi-rigid surfaces, modeling of midsize loudspeakers in the interior of an vehicle is reported on, as well as modeled results for a specific case are given.

1. INTRODUCTION

From previous physical experiments by Shively and House [1], a general set of guidelines were derived for the optimal placement of a loudspeaker in an automotive instrument panel.

The guidelines were derived from frequency response measurements and energy time curves captured in a mock-up of a vehicle windshield and instrument panel. It was seen that as the angle between the windshield and the loudspeaker became smaller (<75°), the mid- and high-frequency SPL increased due to reflections off the windshield. The response smoothness became irregular as the angle became smaller due, in part it was assumed, to comb filtering effects. Also, there is a small (≈ 2 dB) increase in the frequencies below 400 Hz due to boundary reinforcement.

From the energy time curves, it was seen that as the windshield angle became smaller, more energy was reflected back toward the listener. Also, the reflection amplitude became larger and the separation between the direct and reflected energy peaks became smaller. Between 55° to 90° there is a general broadening of the initial energy peak as multiple reflections were fused together to form a bundle of sonic information. For angles less than 70°, the amplitude of the direct energy was smaller than that of the reflected energy. At 55°, the angle is so small that the initial peak and first reflections were fused together to yield a more ideal looking impulse but with a reduced decay envelope slope beyond 7 ms due to the increased reflection energy density.

There was good correlation between the objective and subjective results for this portion of the experiment. There was significance to the mid- and high-frequency balance that can be attributed to a high-frequency accentuation for smaller angles and a high-frequency roll-off for the larger angles. A perceived change to the timbre is caused by the mid-high frequency accentuation and comb filtering effects which adds harshness to the sound quality. The treble balance drove the overall preference and spatial quality for the driver's position.

The conclusion from that portion of the experiments was that for instrument panel mounted loudspeakers, smaller windshield angles (< 55°) and a location closer to the windshield (forward) is preferred for the best overall results but the upper door was a very close second.

Further work determined that "if midranges are placed in the instrument panel, usually the most optimal location is one that is within a distance between the loudspeaker to the apex of the windshield and instrument panel equal to one loudspeaker diameter." Shively [2, 3]

The general set of guidelines that were derived are summarized in the Appendix (§ 8.1) of this paper.

While they seem intuitive, the general guidelines cannot be extrapolated without regard to the influences of additional boundaries, and thus they leave room for interpretation on occasion. An example would be when the compensation for the orientation of the loudspeaker becomes so great as to cause additional boundary effect problems. There are combinations of the loudspeaker's distance from local boundaries and its relative orientation to the windshield angle that don't follow the form of the guidelines completely and need to be modified empirically during development of the vehicle and the audio system, if possible. More often than not, it isn't possible. Usually the only time it is possible to modify a mounting is before development begins, before the automotive CAD data is finalized.

As it is stated in the Appendix (§8.2), given the complexity of the sound field, it is very difficult to provide an accurate theoretical model to predict behavior from instrument panel loudspeaker placement, let alone a simple theoretical equation that will serve as a guideline for loudspeaker placement. That is why an empirical guideline has been used. The analytical sophistication required to properly predict all of the boundary effects is developing, and is the topic of this study.

Furthermore, the purpose of this study is to determine the validity of those original best practice guidelines for the positioning of instrument panel midranges and to set the stage for the analysis of such complex sound fields as common place.

This paper will follow an outline that describes the framework of the process used to obtain an accurate model of the vehicle interior and to show early results from the models.

The geometry for the vehicle interior comes from CATIA CAD data; in this case, it is that of a sedan vehicle. That data is the basis of the acoustic mesh. There are two acoustic solution techniques that are used. The lower frequency part of the frequency response in the simulation result is calculated by a wave expansion technique and the upper frequency part by a ray launching algorithm.

The first model will use characteristic boundary conditions, with no model updates. The second model is derived from a model update procedure for low- and high-frequencies that involves the results from the first model and measured data from the vehicle.

The larger scope of the study will be to find optimal locations for midranges and tweeters in instrument panels, doors, rear decks, and any of the pillar locations available in the automotive interior. For the instrument panel, the locations of interest are the left, right, and center. To test the validity of the process, we began with a simulation of a loudspeaker in the center channel location on the instrument panel and a simple optimization of its location and angle of orientation.

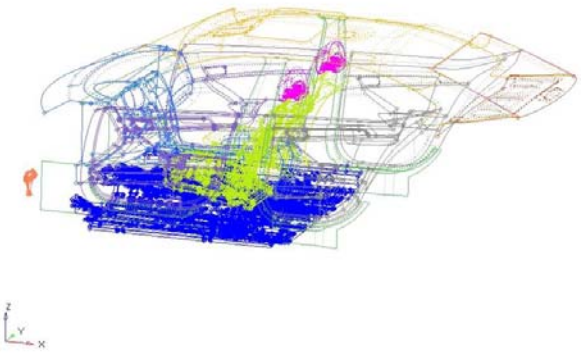

Figure 1 CATIA CAD data of Sedan Vehicle

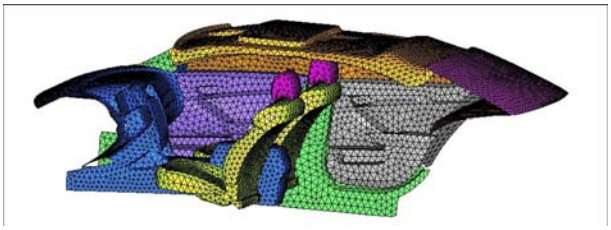

Figure 2 Low-Frequencies, Wave Expansion Acoustic Mesh, derived from CATIA data

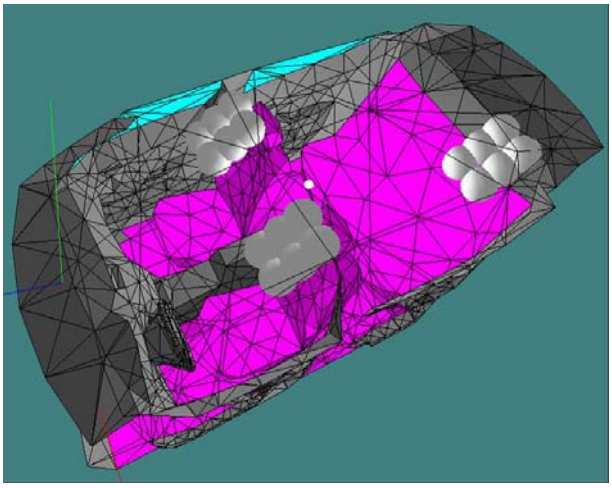

Figure 3 High-Frequencies, Ray Launching, Acoustic Mesh with receiver solution points (mics) depicted by spheres. Loudspeaker is located at the origin of the axes.

2. FIRST MODEL

2.1. Cabin Geometry

The geometry of the sedan vehicle is the basis for the acoustic mesh. No model update is applied. Characteristic boundary condition values are used instead.

The Acoustic mesh is derived from CATIA CAD model of the vehicle. [Figure 1]. Both the low-frequency model and the high-frequency model use the same CAD model as the starting point, but they require different meshes due to the different numerical schemes used. The low-frequency model covers frequency 100 - 1,000 Hz, while high-frequency model is used from 1,000 - 20,000 Hz. The mesh for the low-frequency model is shown in Figure 2. The mesh for the high-frequency model is shown in Figure 3. In the high-frequency model, the locations for acoustic receivers, theoretical microphone locations are displayed.

2.2. Loudspeaker location

For this sedan, it had an existing center channel location which we could easily model and measure. Shown in Figures 4a,b.

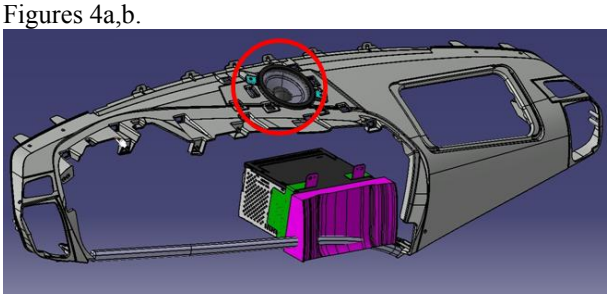

Figure 4a Center Loudspeaker Location

Figure 4b Center Loudspeaker Location

An example of the three-dimensional acoustic results form the low-frequency model are shown in Figure 5.

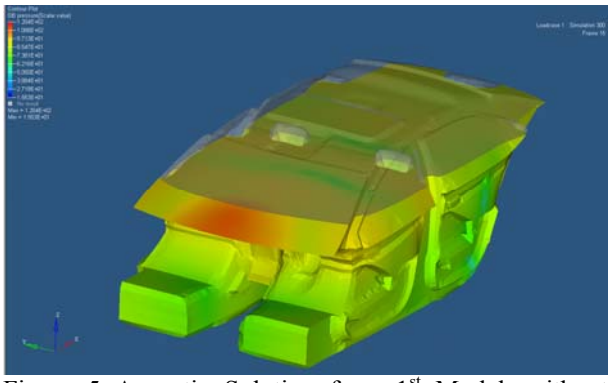

Figure 5 Acoustic Solution from 1st Model, without model update.

3. SECOND MODEL

The second model will perform a model update using measured data and the first model

3.1. In-Vehicle Measurements

3.1.1. Measurement Methods

As stated before, the lower frequency part of the frequency responses of the simulations is calculated by a wave expansion technique and the upper frequency part by a ray launching algorithm. The algorithms are based on different input data: the wave expansion method utilizes the frequency response and the ray launching method utilizes the impulse responses.

To guarantee a measurement with high accuracy for each simulation method an optimised measurement method is used. We consider that the loudspeaker and vehicle cabin embodiment is a time invariant system with a transfer function. This transfer function is assumed to have a large linear part. The loudspeaker is excited at a low voltage level hence minimizing non-linear distortions.

For data utilized in conjunction with the high frequency simulation technique, measurements were performed with a logarithmic sweep as a test signal. This technique was introduced by Angelo Farina [4]. It provides the impulse response and is quite fast and robust.

For measurement data utilized in conjunction with low frequency simulation technique, a coherent stepped sine technique was used. This is a very robust technique as only noise of the currently measured frequency bin is involved in the measurement; see Mueller and Massarani [5]. During the measurement, tracking the nonlinear distortion and the SNR makes it simple for the user to figure out if a part of the measurement chain is not working well.

3.1.2. Sensors

The velocity of the cone is monitored with an accelerometer attached to the dustcap [Figures 6, 7]. Excitation voltage is probed at the driver's terminals. To scan the soundfield inside the cabin, a purposely built 12-microphones array and carrier embodiment was used [Figure 8]. The microphones used are small to minimize the impact on the soundfield and are close to omni-directional.

3.1.3. Positions of the microphones

Each microphone position inside the cabin is referenced to some characteristic points in the vehicle. Special attention is paid to the positions of the seats and the head-rests in order to replicate it inside the models.

SPL was measured in this vehicle at more 100 locations. Because of the massive number of measurement points inside the cabin, this data gathering exercise has been entitled the "100+ measurements". A sample of the measured frequency responses are depicted in Figure 9.

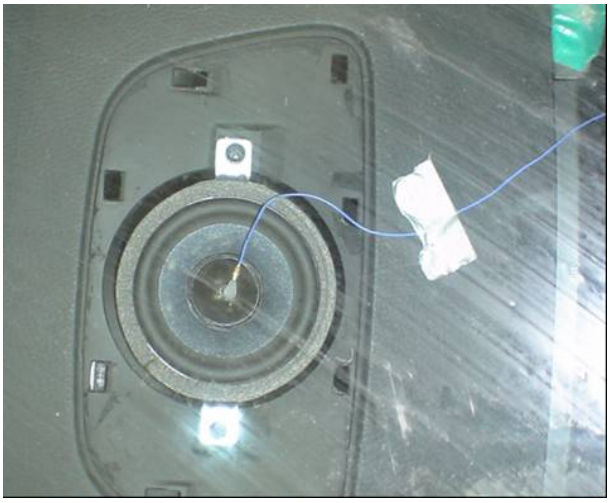

Figure 6 In-Vehicle Cone Velocity Measurements

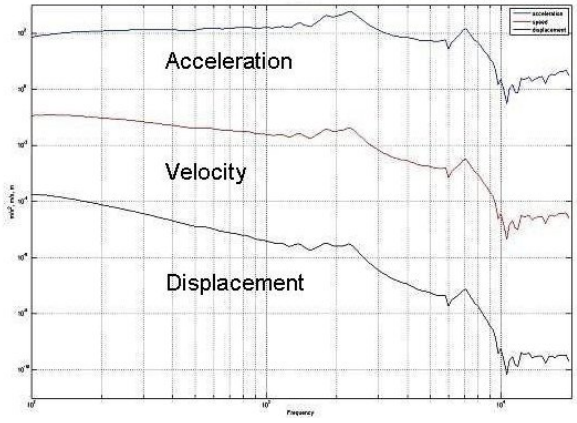

Figure 7 In-Vehicle Cone Acceleration, Velocity, and Displacement vs. Frequency

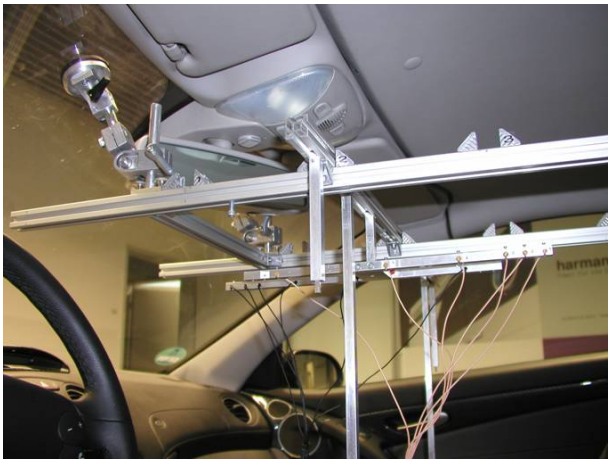

Figure 8 12-microphones array and carrier embodiment.

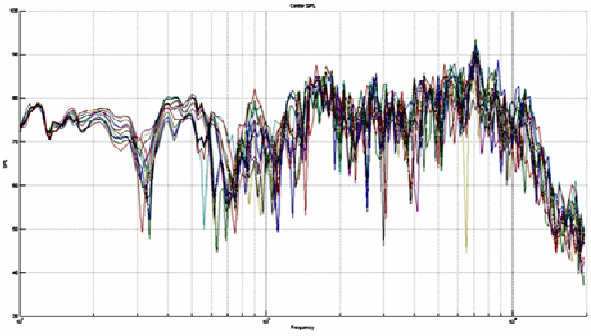

Figure 9 In-Vehicle SPL vs. Frequency from 100+ Microphone Measurements

3.2. Model Update

The model update procedure combines the 1st model results and 100+ measurements to determine appropriate acoustical properties of the interior and more accurate acoustical model of the cabin. The update procedure consists of an optimization loop. During the process, the model parameters are varied following a particular optimization scheme. The optimizer tries to minimize the error between the current model and a set of SPL measurements.

3.2.1. Error Calculation

Each SPL value is considered as a point in the Cartesian plane thus it's possible to calculate the aggregated normalized spatial distance between the target SPL and the calculated SPL. The target SPL (SPL_T) and calculated SPL (SPL_C) are defined as:

$$SPL_T = A_T(\cos(\alpha_T) + i\sin(\alpha_T))$$
$$SPLc = A_c(\cos(\alpha_c) + i\sin(\alpha_c))$$

where A_T and A_c are the absolute values of the target and calculated SPL and α_T and α_c are the angles of the pressure. The aggregated error E is defined as:

$$E = \frac{1}{N}\sqrt{\sum_{l=1}^{l=N}(A_{Tl}\cos\alpha_{Tl} - A_{cl}\cos\alpha_{cl})^2 + (A_{Tl}\sin\alpha_{Tl} - A_{cl}\sin\alpha_{cl})^2}$$

3.2.2. Updating Procedure

The updating procedure depends on a specified search range symmetric and centered to a complex material initial impedance value. Defining N and W the number of iterations and the impedance increment, the search range is equal to (2N+1)*W. The user has to specify an initial impedance value Z_{in}, thus the tested Z_t impedance values will be defined as:

$$Z_{ti} = Z_{in} + (i - N) * W \qquad \text{for } 0 \le i \le 2N$$

The vehicle cabin model is based on an impedance number N_Z, thus the updating procedure is launched $2*N_Z$. For each updating procedure, the impedance value used for the next iteration will correspond to the minimum error E.

To optimize the model update performances, the N iterations optimization process can be launched L times (L is the number of loops). For each loop, if the optimized solution corresponds to the lower (or upper) edge of the range, the search range needs to slide downwards (upwards) with an overlapping the two points, and the value W is not modified. If the optimized solution is not on the upper or lower edge, the W value is divided by the factor N.

For a model based on N_Z materials, L loops and N iterations, the model will be launched 2*(2N+1)*L*N times.

3.2.3. Process Description

The optimization process is structured in a way to enable it to be used by any of the numerical kernels proprietary to Harman International but also by any commercial solver. The input and output optimizer files are ASCII files. The optimization process procedure is described in Figure 10.

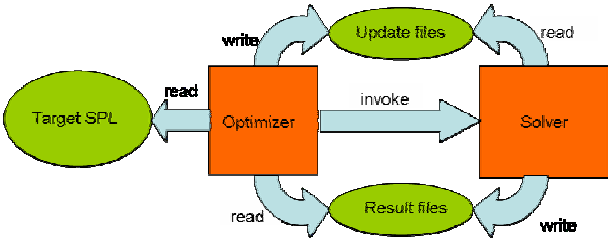

Figure 10 Model Update Optimization Process Procedure

4. THIRD MODEL

4.1. Investigated Loudspeaker Locations and Angles

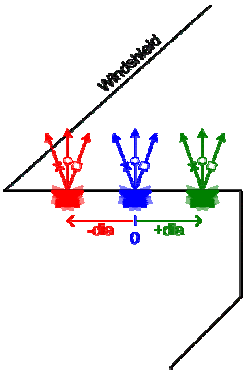

CFG	POS	AIM(°)
0	0	0 (○)
1	0	-10 (□)
2	0	+10 (x)
3	+dia	0 (○)
4	+dia	-10 (□)
5	+dia	+10 (x)
6	-dia	0 (○)
7	-dia	-10 (□)
8	-dia	+10 (x)

Figure 11 Center Midrange Positions and Angles

The location of the midrange, as shown in Figure 11, was modeled in the existing location from the CAD data (config 0) and at locations one diameter closer to the apex of the windshield and the instrument panel and one diameter farther away. The second part of each configuration was the aiming angle, or orientation, of the loudspeaker. It was either at no change from the position in the CAD data, -10º (away from the windshield), or +10º (toward the windshield).

The anechoic data for the midrange that was to be modeled as the source is shown in Figure 12.

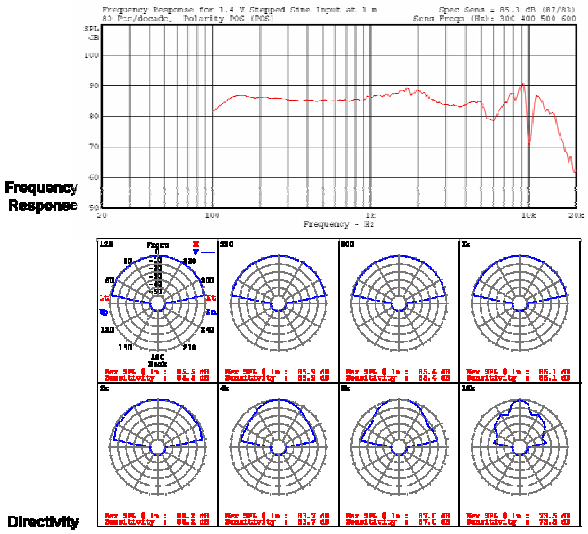

Figure 12 On-Axis Anechoic Frequency Response and Directivity of the Source.

4.2. Low-Frequency Model

Low-frequency modeling is based on a full domain discretization approach. The cabin volume is meshed with tetrahedral elements and a solution is found by numerically approximating the steady-state Helmholtz equation at each mesh point.

The solution thus obtained assumes transient effects have vanished. The acoustic field at each mesh point then varies harmonically with time.

To obtain a numerical approximation of the acoustic field, several techniques may be used. For this project, a highly accurate wave expansion approach – several times more efficient than commercially available tools – was implemented.

The optimized complex frequency-dependent impedances obtained with the model update were used directly in the simulation model to prescribe the boundary conditions. From the definition of the impedance:

$$z = \frac{p}{u},$$

It is possible to obtain a relationship for z in terms of either p or u using:

$$\frac{\partial p}{\partial n} = -\rho \frac{\partial u}{\partial t},$$

where ρ is the air density and n is a vector normal to the boundary surface at each boundary discretization point.

The excitation from the source was applied in a similar fashion with the loudspeaker modeled as a flat piston located in the same position as the actual loudspeaker. Since the air particles move at the same speed as the piston at the interface, the measured cone accelerations were integrated and then applied using the equation above.

Some example results from the low-frequency model are shown in Figures 13 a, b.

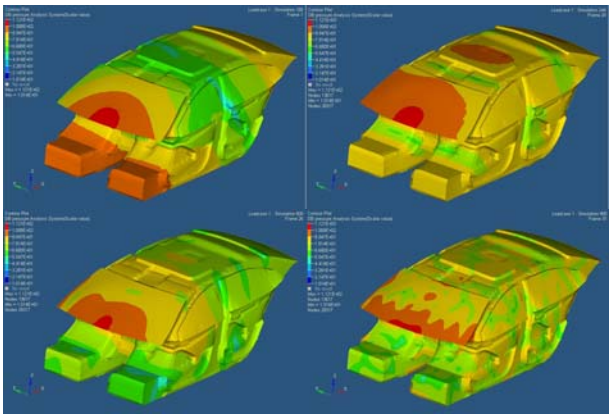

Figure 13a Low-Frequency Model Result for Config 0: 100Hz, 244Hz, 500Hz, and 900Hz (clockwise).

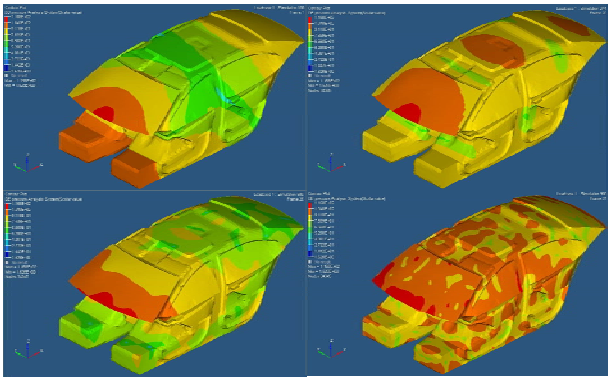

Figure 13b Low-Frequency Model Result for Config 7: 100Hz, 244Hz, 500Hz, and 900Hz (clockwise).

4.3. High-Frequency Model

The high-frequency model utilizes a simulation technique based on Geometrical Acoustics (GA).

4.3.1. Introduction to Geometrical Acoustics

GA assumes a high mode density. A high modes density yields a high likelihood of a diffuse field. It is typically considered that this criterion is full-filled when at least three modes can be excited within their respective half-power points for any frequency under study. The threshold is known as the Schroeder frequency. Above this frequency, the energy propagates mainly along specular paths (i.e. like light) and then Snell's law applies. When hitting a surface, the energy is then: a) absorbed; b) reflected; and c) scattered.

There are several approaches in GA modeling. The historical approach is a fully deterministic calculation of all image sources relative to all planes in the geometry. This approach is called the Image Source Model (ISM). [Figure 14.] It is accurate but requires an exponentially increasing computation time as the reflection order increases. An alternate approach is a stochastic launch of rays or cones in all directions around the source. Rays/cones collected at the receiver location then define a valid path. [Figure 15.] This approach is efficient in terms of computation time but some paths might be missed. Different commercial packages are available using one of the two approaches, or combination of both. We are using a hybrid approach that combines ISM for first orders reflections; and Rays Launch for higher orders.

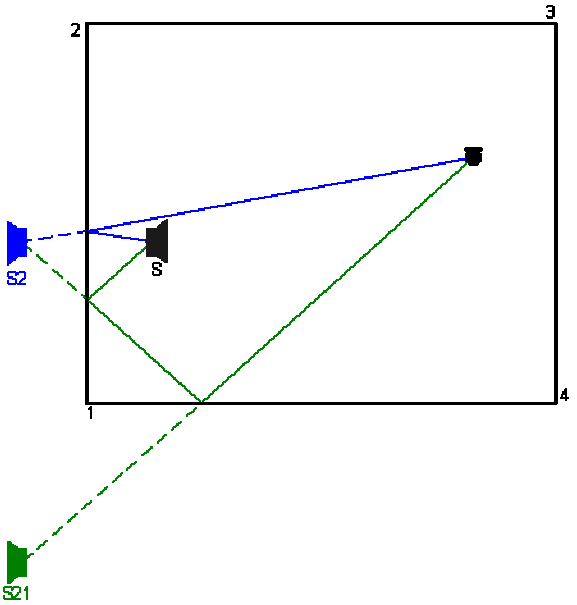

Figure 14 ISM Approach

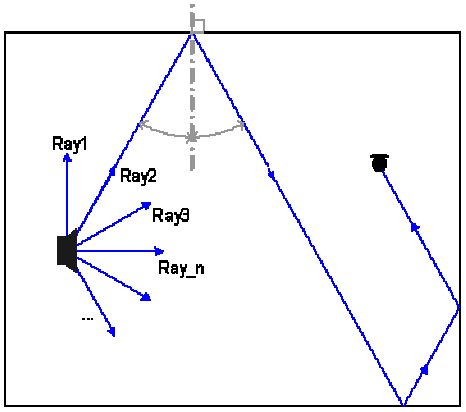

Figure 15 Random Rays Launch Approach

4.3.2. Inputs

Cabin geometry: The GA model mesh is an altered, simplified version of the low-frequency mesh featuring a relevant level of details. The mesh includes also the position of the different source(s) and receiver(s) as well as their orientation.

Source(s) characterization: The source is defined by its on-axis anechoic response and its directivity.

Material characterization: Each material type is defined by its absorption and scattering properties in each eight octave bands from 125Hz to 16 kHz. These parameters are derived during the model update procedure.

4.3.3. The Model

The cabin interior modeled here has been meshed with 1,500+ elements. There are 18 receivers/microphones – i.e., an array of six microphones located at the front left, front right and rear left seat. The loudspeaker is defined as a source flush mounted on the instrument panel. The source is moved and angled to investigate different mounting options. Due to the volume of the cabin, we are investigating frequencies at 1 kHz and higher. An example of the Rays launch results is given in Figure 16.

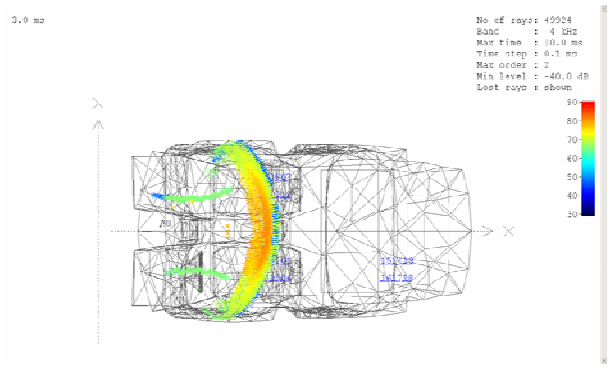

Figure 16 High-Frequency Model Result example

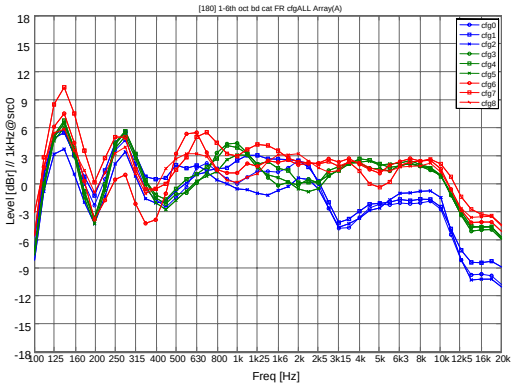

Figure 18 Concatenated Frequency Responses at Array Position (A) Front Driver

5. COMBINED RESULTS

The end results [Figures 18, 19, 20] are shown as typical SPL response versus microphone location. The low frequency frequency-step animations give a full understanding of the sound pressure distribution throughout the vehicle at frequencies below 1 kHz. As well, in the high frequency time-step animation of the non-optimal loudspeaker configuration and the optimal configuration, it is easy to see the non-uniformity of the sound propagation and numerous reflections influencing that sound field. It is the non-uniformity that is key to seeing the optimal location. The influence of the loudspeakers location and the boundary conditions is seen in the reflections.

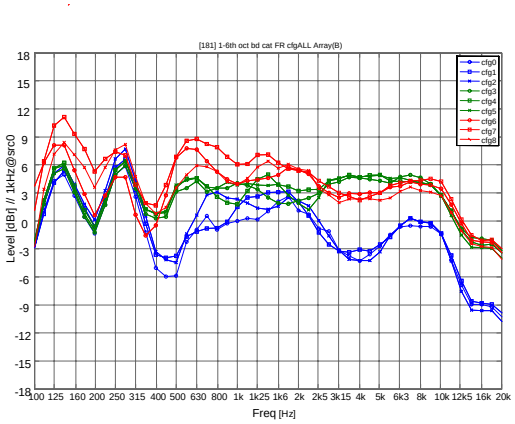

Figure 19 Concatenated Frequency Responses at Array Position (B) Front Passenger

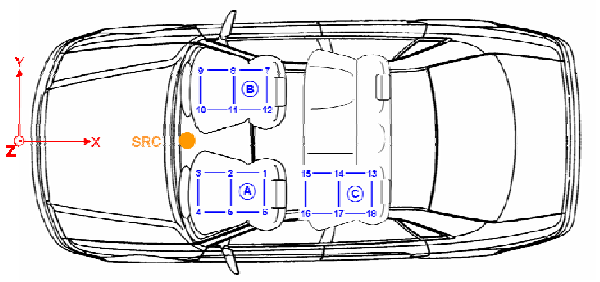

Figure 17 Microphone Array Positions A, B, and C for Simulation Results.

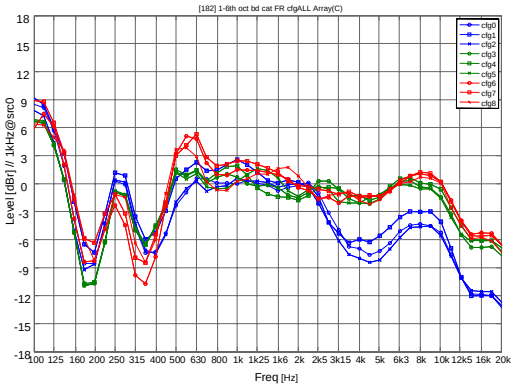

Figure 20 Concatenated Frequency Responses at Array Position (C) Left Rear Passenger

6. CONCLUSIONS

- Position of loudspeaker has clear impact on frequency response
- Blue positions display strong interferences between 3 and 5 kHz
- Blue pos radiates less high-frequency energy
- Red & green position present similar features above 4 kHz
- Red position gives better loading below 3 kHz for both front seat positions
- In rear seat, the modal behavior of the vehicle interior is clearly displayed
- Among red positions, the square configuration gives an even slightly better loading below 2 kHz and would probably be preferred for it overall consistency.

The results are consistent with what is experienced empirically and encourage us to continue with the larger scope of the study. From these preliminary results, it would appear we could make more informed decisions using this computer aided model approach than by using the general guidelines previously employed.

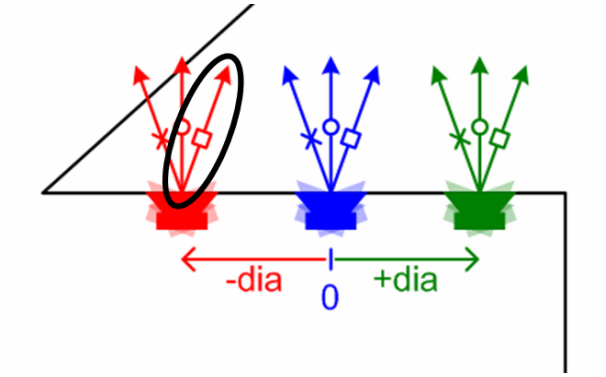

Figure 21 Optimal Loudspeaker Configurations from Simulation, with the potential best configuration circled.

7. REFERENCES

[1] R.E. Shively, W.N. House, "Perceived Boundary Effects in an Automotive Vehicle Interior", Presented at the 100th Conv. of the AES, Copenhagen, (1996 May), Preprint 4245.

[2] R.E. Shively, "Automotive Audio: System Engineering", Presented to the AES Los Angeles Section, (1999 March).

[3] R.E. Shively "Automotive Audio Design (A Tutorial)", Presented at the 109th Conv. of the AES, Los Angeles, (2000 September), Preprint 5276

[4] A. Farina, "Simultaneous Measurement of Impulse Response and Distortion with a Swept-sine technique", Presented at the 108th AES Convention, Paris 2000, Preprint 5093

[5] S. Mueller, P. Massarani, "Transfer-Function Measurement with Sweeps", Director's cut, http://www.melaudia.net/zdoc/comparisonMesure.PDF, July 2009-07-21

8. APPENDIX (PRIOR ART)

8.1. General Instrument Panel Loudspeaker Location Guidelines (derived from Shively [1], [2], [3])

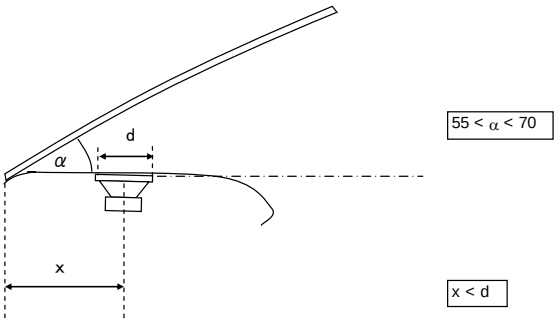

Figure 22 Windshield, Instrument Panel, Loudspeaker Example

8.1.1.

8.1.2. Loudspeaker Location

For best sound quality, the distance (x) from the windshield baseline to the centerline of a loudspeaker located in the instrument panel should be at least one loudspeaker diameter (d).

8.1.3. Loudspeaker/Windshield Orientation Angle

For best sound quality, the angle (α) between the windshield and the loudspeaker-mounting plane should be between 55 º and 70 º.

If the angle is less than 55 º, the loudspeaker distance should move backward (away from the windshield) by a proportional amount or angled away from the windshield.

The larger the angle gets from 55 º toward 70 º, the more the loudspeaker should be angled toward the windshield. The loudspeaker should never be placed in a plane that is parallel with the windshield.

8.2. Theoretical Acoustical Comb Filtering and Measured Frequency Response

Comb filtering is result of two identical signals separated by some phase being recombined. When they are recombined in phase, the amplitude is doubled (+6dB) [Figure 23]; when they are 180 º out of phase, they cancel leaving a deep null. With proper placement, a loudspeaker reflecting off of a nearby surface can have a very dense packing of comb filtering, and minimize the audible distortion crated by it. Figure 24 below shows that, in theory, a loudspeaker one cone diameter away from a windshield surface minimizes the destructive nature of comb filtering, over most of its useful mid- and high-frequency range. It is also illustrated in Figures 25, 26 how spacing of more than one diameter can cause a level of comb filtering that is audible as coloration and distortion.

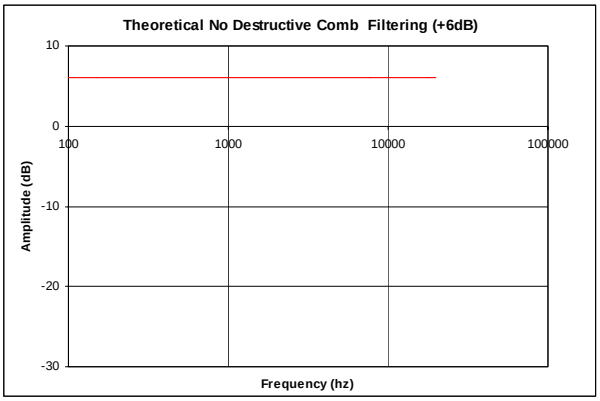

Figure 23 Theoretical No Destructive Comb Filtering (+6dB)

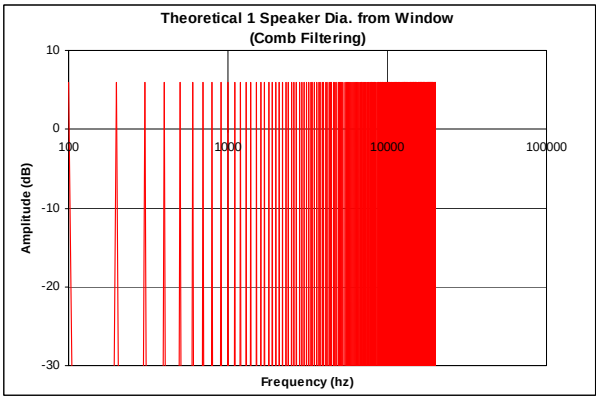

Figure 24 Theoretical 1 Loudspeaker Dia. From Windshield

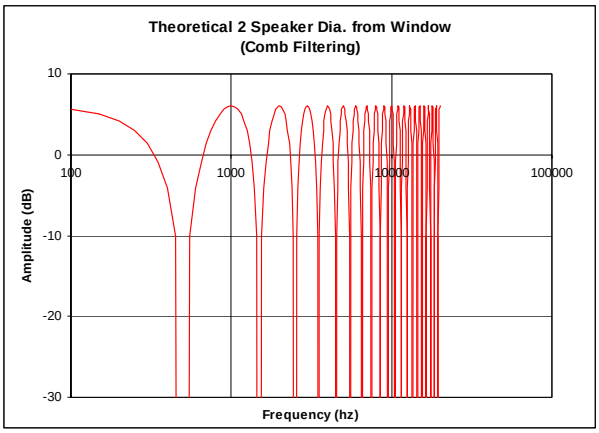

Figure 25 Theoretical 2 Loudspeaker Dia. From Windshield

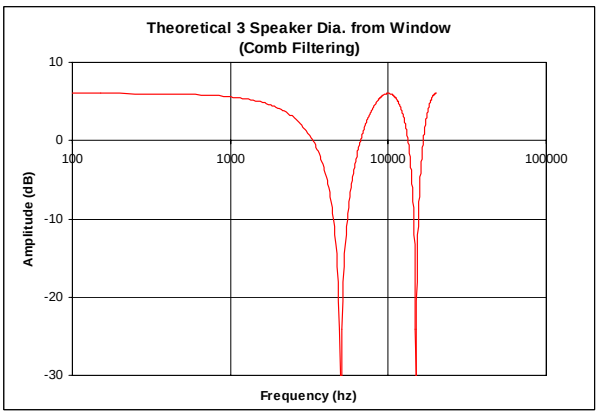

Figure 26 Theoretical 3 Loudspeaker Dia. From Windshield

Comb filtering is just one of the influences on the acoustical response of a loudspeaker placed in the IP. Diffraction from nearby trim features is another. The theoretical results assume a single reflective surface with no subsequent reflections. The subsequent reflections which happen in an actual application will have additional phase shifts creating separate wavefronts which will combine with the previous wavefront and so on. This will continue to compound the complexity of the resultant wavefront that is delivered to the listener. In addition to those boundary effects local to the loudspeaker, there are the early reflections from boundaries nearby the listener's head position: Door window glass, steering wheel, headrest, top of seat back, and listener's shoulders to name a few.

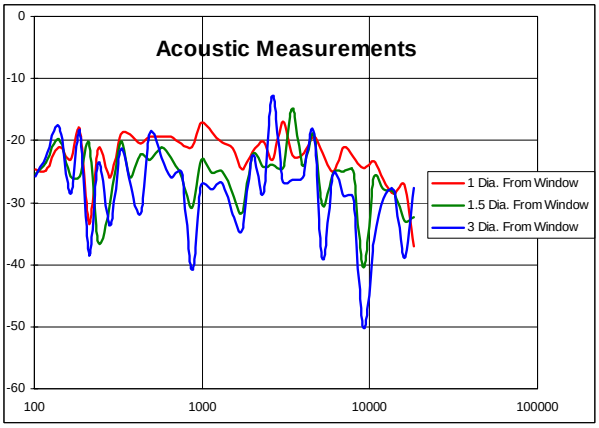

Figure 27 Measurements made with Windshield Angle @ 55º, Shively and House [1]

Given this complexity of the sound field, it is very difficult to provide an accurate theoretical model to predict behavior from IP loudspeaker placement, let alone a simple theoretical equation that will serve as a guideline for loudspeaker placement. That is why an empirical guideline has been used and continues to be used until the analytical sophistication required to properly predict all of the boundary effects is developed. That is the purpose of present study.